Available online at www.sciencedirect.com

ScienceDirect

Mendeleev Commun., 2024, **34**, 478–480

Mendeleev Communications

Composite cathode material based on sulfur and microporous carbon for Li–S batteries

Svetlana A. Novikova,[a] Daria Yu. Voropaeva,[a] Sergey A. Li,[b] Tatiana L. Kulova,[b] Alexander M. Skundin,[b] Irina A. Stenina[a] and Andrey B. Yaroslavtsev*[a]

[a] *N. S. Kurnakov Institute of General and Inorganic Chemistry, Russian Academy of Sciences, 119991 Moscow, Russian Federation. E-mail: yaroslav@igic.ras.ru*

[b] *A. N. Frumkin Institute of Physical Chemistry and Electrochemistry, Russian Academy of Sciences, 119071 Moscow, Russian Federation*

DOI: 10.1016/j.mencom.2024.06.003

In this work, a new cathode material for lithium–sulfur (Li–S) batteries was developed. Microporous carbon (with predominant pore size ⩽1.2 nm) served as both a matrix for sulfur retention and conductive additive. Microporous carbon was shown to be capable of adsorbing lithium polysulfides thereby suppressing their migration toward lithium anode. The discharge capacity of the S/C composite at the 1st and 20th cycles in Li–S battery operation was 513 and 421 mAh g^{-1} at a scan rate of 0.1 mV s^{-1}.

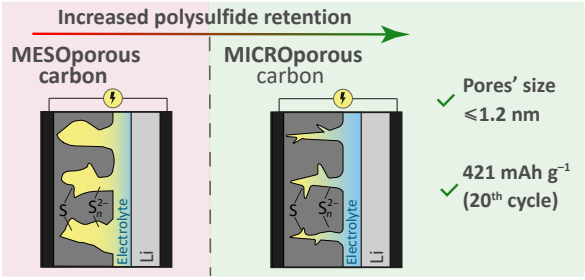

Keywords: Li–S battery, cathode material, sulfur, microporous carbon, adsorption, lithium polysulfides.

Li–S batteries are considered as a promising alternative for lithium-ion batteries due to their high energy density and low cost of sulfur-based cathodes.[1–3] The theoretical specific energy density of Li–S batteries is significantly higher than that of Li-ion batteries (~2500 and ~420 Wh kg^{-1}, respectively).[4] Generally, a Li–S battery consists of a lithium metal anode, lithium-conductive electrolyte, and a composite sulfur cathode.[2,5,6] In sulfur cathodes, Li^+ and electrons are intercalated into the material structure, forming lithium polysulfides (Li_2S_n, $2 \leqslant n \leqslant 8$) or lithium sulfide ($Li_2S$).

Reduction reactions generating solid Li_2S_2 and Li_2S are characterized by poor kinetics and the theoretical capacity of Li–S batteries cannot be achieved.[7–14] The practical application of Li–S batteries is limited by several issues including the safety of metallic lithium as anode, low electrical conductivity of sulfur (5×10^{-30} S cm^{-1}) and the discharge products (Li_2S_2/Li_2S),[15–17] a significant volume change of the cathode during the charge/discharge processes, formation of polysulfides (Li_2S_n, n = 4–8) soluble in the electrolyte and their migration towards the anode (shuttling) with subsequent irreversible reactions resulting in the loss of active material.[2,7] One of the main challenge is to eliminate shuttling of polysulfides.[8,19]

A promising approach is to obtain composites based on sulfur and meso- and/or microporous carbons with a hierarchical porous structure capable of both providing electron transfer and encapsulating sulfur, suppressing the dissolution and migration of polysulfides.[1,2,5,7,9,20–26] Due to the limited pore space in such composites, n in sulfur molecules S_n is usually 2–4, which prevents the formation of soluble long-chain polysulfides.[1] It should be noted that although intermediate polysulfides are thermodynamically unstable in the solid state, their formation is possible due to their solvation by the electrolyte.

In this work, we developed and investigated a novel cathode material based on sulfur composite with microporous carbon with a predominant pore size ⩽1.2 nm, which, on the one hand, can provide electrical conductivity and, on the other hand, retain the products of sulfur reduction in the cathode.

Microporous carbon was obtained by the technique reported earlier.[27] (see details in the Online Supplementary Materilas).

According to SEM images, the microporous carbon represents particles of ~20 μm in size. The morphology of the composite with sulfur is similar to the original microporous carbon [see Online Supplementary Materials, Figure S1 (*a*–*d*)]. Backscattered electron SEM images of the S/C composite indicate a uniform distribution of sulfur in the composite [Figure S1 (*e*,*f*)].

The specific surface area was found to be 2623 m^2 g^{-1}. The predominant pore size is ~0.8–1.2 nm (Figure S2). The total pore volume is ~1.29 cm^3 g^{-1}, which corresponds to a possible sulfur loading of up to 73 wt%. The specific surface area of the S/C composite was 2 m^2 g^{-1}. A sharp decrease in the surface area after sulfur loading indicates that sulfur occupies almost the entire pore volume of microporous carbon or blocks the access of nitrogen into them.

A broad halo with a maximum in the region of 2θ <10°, which corresponds to interplanar distances comparable to the pore size, can be noted in the XRD pattern of microporous carbon. In the S/C composite, a broad halo is shifted to the region 2θ ~22–30° and corresponds to the position of the most intense sulfur reflexes (Figure S3), which may be due to a decrease in the size of sulfur particles and/or its amorphization. At the temperature of the S/C composite synthesis (155 °C), liquid sulfur has the lowest viscosity and is represented mainly by cyclic molecules S_8.[28] Sulfur molecules can diffuse into micropores, and their crystallization is hindered by the low pore volume.

The intense peaks with maxima at 1599 and 1344 cm^{-1} in the Raman spectrum of the microporous carbon (Figure S4) can be attributed to the G- and D-bands of graphite.[29,30] The contribution of these bands to the integral intensity of the

spectrum is 43% [Figure S4(*b*)], which is consistent with the rather high electronic conductivity of microporous carbon (~5.3×10^{-2} S cm^{-1}).[31] In addition, two more broad peaks can be observed at ~1290 and ~1540 cm^{-1} (Figure S4), corresponding to other carbon species.[31] There are no typical sulfur peaks in the Raman spectrum of the S/C composite [Figure S4(*a*)], which most probably corresponds to its disordering or almost complete incorporation into the carbon pores. The electrical conductivity of the S/C composite is 9.9×10^{-5} S cm^{-1}.

The ability of carbon to adsorb lithium polysulfides is an important property for the composite S/C cathode because it helps to suppress the migration of polysulfides toward the anode. The polysulfide adsorption test was performed by addition of dilute Li_2S_6 solution to the microporous carbon (Figure 1). For comparison, the same experiment was performed for mesoporous carbon investigated by us earlier.[32] When 1 ml of 0.003 M Li_2S_6 solution (3 μmol) was added, the solution color disappeared after shaking and sedimentation of both microporous and mesoporous carbons. When the amount of polysulfide was increased up to 13.5 μmol, a slight coloring of the solution was observed over the mesoporous carbon [Figure 1(*b*)], while the solution over the microporous carbon remains colorless. The obtained data indicate that microporous carbon shows greater sorption ability to lithium polysulfides compared with mesoporous carbon.

Figure 2(*a*) shows the CV for the 1st, 5th and 20th cycles in the potential range of 1.4–3.0 V. At the first cycle, there is a slight decrease in capacity, but then the S/C cathode shows stable cycling [Figure 2(*b*)].

Except for the 1st cycle, where wide maxima are observed and the reduction and oxidation peaks are slightly shifted, the shape of the cathodic curves remains relatively constant during cycling. From the 2nd cycle onwards, two cathodic and one anodic maxima can be identified in the CV curves, with potential regions consistent with data reported.[2,11,13,33–36] The S/C electrode shows typical discharge behavior in ester-based electrolyte (dioxolane + dimethoxyethane). According to the data available in the literature, the first peak with a maximum at ~2.3 V corresponds to the conversion from sulfur to S_n^{2-} polysulfide dianions (where n = 6–8), while the second peak at ~2.0 V is associated with the conversion of polysulfides to Li_2S_n (where n = 2–4) and Li_2S.[25] The obtained S/C composite differs in electrochemical behavior from composites based on ultramicroporous carbon and is more similar to composites based on mesoporous carbons.[25,37] In our case, there is no significant charge/discharge potential hysteresis. The pore size of ~0.8–1.2 nm is sufficient for the penetration of ester solvent molecules and redox reaction in the investigated S/C composite at the three-phase boundaries of sulfur, carbon and electrolyte molecules coexistence. The capacity loss during cycling turns out to be noticeably less compared with the composite based on mesoporous carbon[32] as a result of better polysulfide intermediates retention because of their adsorption in micropores.

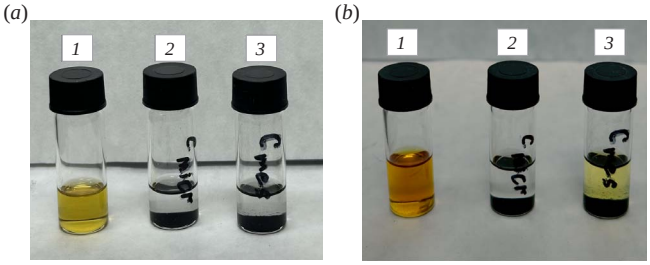

Figure 1 Photographs of (*1*) Li_2S_6 solution and the same solution in contact with (*2*) microporous and (*3*) mesoporous carbon. Amount of Li_2S_6: (*a*) 3 and (*b*) 13.5 μmol.

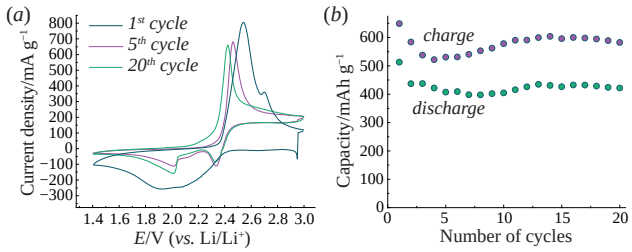

Figure 2 (*a*) CV of S/C|Li cells and (*b*) charge and discharge capacities over 20 cycles.

As the cycling continues, the intensity ratio of the cathode peaks changes [Figure 2(*a*)]. The intensity of the peak with a maximum at ~2.3 V decreases, while the peak with a maximum at ~2.0 V, on the contrary, increases from the 5th to the 20th cycle. It can be assumed that during cycling the dissolution and removal of long-chain polysulfides from larger pores (2–3 nm in size) with a weaker adsorption take place, though their amount is not significant (see Figure S2).

The discharge capacity at the 1st cycle is 513 mAh g^{-1}. This value is less than the theoretical one, which is due to a rather high rate of sweep potential during CV measurements (0.1 mV s^{-1}), which corresponds to the C-rate of ~C/2. At further cycling, the capacity goes through a minimum and slightly increases to 421 mAh g^{-1} by the 20th cycle. The electrochemical characteristics of the obtained cathode material are noticeably superior to those of the cathodes obtained by mechanical mixing of sulfur with carbon material[38] and also show greater stability during cycling compared to mesoporous carbon-based composite.[32] There is no decrease in the discharge potential as in the case of ultramicroporous carbons with pore sizes of < 0.7 nm.[39,40]

To improve Li–S battery performance, a novel cathode material based on the composite of sulfur with microporous carbon was developed and investigated. Its structural, morphological and electrochemical characteristics were studied. Cathodes based on the obtained composite have demonstrated an increased stability during cycling, which was explained by the proper pore size distribution in microporous carbon and its ability to sorb lithium polysulfides.

This work was financially supported by the Russian Science Foundation (grant no. 23-19-00642), https://rscf.ru/project/23-19-00642/.

This research was performed using the equipment of the JRC PMR IGIC RAS.

Online Supplementary Materials

Supplementary data associated with this article can be found in the online version at doi: 10.1016/j.mencom.2024.06.003.

References

1 S. Xin, L. Gu, N.-H. Zhao, Y.-X. Yin, L.-J. Zhou, Y.-G. Guo and L.-J. Wan, *J. Am. Chem. Soc.*, 2012, **134**, 18510.
2 X. Yu and A. Manthiram, *Adv. Funct. Mater.*, 2020, **30**, 2004084.
3 D. Yu. Voropaeva, E. Yu. Safronova, S. A. Novikova and A. B. Yaroslavtsev, *Mendeleev Commun.*, 2022, **32**, 287.
4 Z. W. Seh, Y. Sun, Q. Zhang and Y. Cui, *Chem. Soc. Rev.*, 2016, **45**, 5605.
5 F. Pei, L. Lin, A. Fu, S. Mo, D. Ou, X. Fang and N. Zheng, *Joule*, 2018, **2**, 323.
6 L. Chen, Y. Yuan, R. Orenstein, M. Yanilmaz, J. He, J. Liu, Y. Liu and X. Zhang, *Energy Storage Mater.*, 2023, **60**, 102817.
7 A. Manthiram, Y. Fu, S.-H. Chung, C. Zu and Y.-S. Su, *Chem. Rev.*, 2014, **114**, 11751.
8 D.-W. Wang, Q. Zeng, G. Zhou, L. Yin, F. Li, H.-M. Cheng, I. R. Gentle and G. Q. M. Lu, *J. Mater. Chem. A*, 2013, **1**, 9382.
9 H. M. Joseph, M. Fichtner and A. R. Munnangi, *J. Energy Chem.*, 2021, **59**, 242.
10 J. Li, L. Gao, F. Pan, C. Gong, L. Sun, H. Gao, J. Zhang, Y. Zhao, G. Wang and H. Liu, *Nano-Micro Lett.*, 2024, **16**, 12.

11 T. L. Kulova, S. A. Li, E. V. Ryzhikova and A. M. Skundin, *Russ. J. Phys. Chem. A*, 2021, **95**, 2138 (*Zh. Fiz. Khim*., 2021, **95**, 1591).
12 L. Ji, M. Rao, H. Zheng, L. Zhang, Y. Li, W. Duan, J. Guo, E. J. Cairns and Y. Zhang, *J. Am. Chem. Soc.*, 2011, **133**, 18522.
13 D. Cai, M. Lu, L. Li, J. Cao, D. Chen, H. Tu, J. Li and W. Han, *Small*, 2019, **15**, 1902605.
14 G. Zhou, H. Tian, Y. Jin, X. Tao, B. Liu, R. Zhang, Z. W. Seh, D. Zhuo, Y. Liu, J. Sun, J. Zhao, C. Zu, D. S. Wu, Q. Zhang and Y. Cui, *Proc. Natl. Acad. Sci.*, 2017, **114**, 840.
15 V. S. Kolosnitsyn and E. V. Karaseva, *Russ. J. Electrochem.*, 2008, **44**, 506 (*Elektrokhimiya*, 2008, **44**, 548).
16 M. Yu, J. Ma, M. Xie, H. Song, F. Tian, S. Xu, Y. Zhou, B. Li, D. Wu, H. Qiu and R. Wang, *Adv. Energy Mater.*, 2017, **7**, 1602347.
17 M. Hakimi and M. Hakimi, *Colloids Surf., A*, 2024, **685**, 133265.
18 A. N. Mistry and P. P. Mukherjee, *J. Phys. Chem. C*, 2018, **122**, 23845.
19 S. A. Novikova, D. Yu. Voropaeva and A. B. Yaroslavtsev, *Inorg. Mater.*, 2022, **58**, 333.
20 B. Zhang, X. Qin, G. R. Li and X. P. Gao, *Energy Environ. Sci.*, 2010, **3**, 1531.
21 Z. Li, L. Yuan, Z. Yi, Y. Sun, Y. Liu, Y. Jiang, Y. Shen, Y. Xin, Z. Zhang and Y. Huang, *Adv. Energy Mater.*, 2014, **4**, 1301473.
22 D.-W. Wang, G. Zhou, F. Li, K.-H. Wu, G. Q. (Max) Lu, H.-M. Cheng and I. R. Gentle, *Phys. Chem. Chem. Phys.*, 2012, **14**, 8703.
23 L. Hu, Y. Lu, T. Zhang, T. Huang, Y. Zhu and Y. Qian, *ACS Appl. Mater. Interfaces*, 2017, **9**, 13813.
24 H. B. Wu, S. Wei, L. Zhang, R. Xu, H. H. Hng and X. W. (David) Lou, *Chem. – Eur. J.*, 2013, **19**, 10804.
25 X. Ji, K. T. Lee and L. F. Nazar, *Nat. Mater.*, 2009, **8**, 500.
26 W. Zhang, D. Qiao, J. Pan, Y. Cao, H. Yang and X. Ai, *Electrochim. Acta*, 2013, **87**, 497.
27 A. V. Melezhik, A. D. Zelenin, O. V. Alekhina, N. R. Memetov and A. G. Tkachev, *Adv. Mater. Technol.*, 2020, **18** (2), 25.
28 B. Meyer, *Chem. Rev.*, 1976, **76**, 367.
29 J. D. Wilcox, M. M. Doeff, M. Marcinek and R. Kostecki, *J. Electrochem. Soc.*, 2007, **154**, A389.
30 R. P. Vidano, D. B. Fischbach, L. J. Willis and T. M. Loehr, *Solid State Commun.*, 1981, **39**, 341.
31 I. A. Stenina, R. R. Shaydullin, A. V. Desyatov, T. L. Kulova and A. B. Yaroslavtsev, *Electrochim. Acta*, 2020, **364**, 137330.
32 A. B. Yaroslavtsev, S. A. Novikova, D. Yu. Voropaeva, S. A. Li and T. L. Kulova, *Batteries*, 2022, **8**, 162.
33 Y.-J. Choi, Y.-D. Chung, C.-Y. Baek, K.-W. Kim, H.-J. Ahn and J.-H. Ahn, *J. Power Sources*, 2008, **184**, 548.
34 J. Cao, C. Chen, Q. Zhao, N. Zhang, Q. Lu, X. Wang, Z. Niu and J. Chen, *Adv. Mater.*, 2016, **28**, 9629.
35 N. Li, F. Gan, P. Wang, K. Chen, S. Chen and X. He, *J. Alloys Compd.*, 2018, **754**, 64.
36 B. Cao, J. Huang, Y. Mo, C. Xu, Y. Chen and H. Fang, *ACS Appl. Mater. Interfaces*, 2019, **11**, 14035.
37 Y. Xiang, L. Lu, Y. Zhang, G. Ersek, G. Portale, W. Li, W. Zhang, A. Kottapalli and Y. Pei, *J. Colloid Interface Sci.*, 2024, **665**, 286.
38 T. L. Kulova, S. A. Li, E. V. Ryzhikova and A. M. Skundin, *Russ. J. Electrochem.*, 2022, **58**, 391 (*Elektrokhimiya*, 2022, **58**, 203).
39 M. Helen, T. Diemant, S. Schindler, R. J. Behm, M. Danzer, U. Kaiser, M. Fichtner and M. Anji Reddy, *ACS Omega*, 2018, **3**, 11290.
40 M. Helen, M. Anji Reddy, T. Diemant, U. Golla-Schindler, R. J. Behm, U. Kaiser and M. Fichtner, *Sci. Rep.*, 2015, **5**, 12146.

Received: 19th March 2024; Com. 24/7429